# Phytoplankton light absorption in the deep chlorophyll maximum layer of the Black Sea

T. Churilova, V. Suslin, H.M. Sosik, T. Efimova, N. Moiseeva, S. Moncheva, V. Mukhanov, O. Rylkova & O. Krivenko

Published online: 24 Oct 2018.

Submit your article to this journal ⬚

Article views: 326

View related articles ⬚

View Crossmark data ⬚

Taylor & Francis
Taylor & Francis Group

# Phytoplankton light absorption in the deep chlorophyll maximum layer of the Black Sea

T. Churilova [a], V. Suslin [b], H.M. Sosik [c], T. Efimova[a], N. Moiseeva[a], S. Moncheva [d], V. Mukhanov[a], O. Rylkova[a] and O. Krivenko[a]

[a]Kovalevsky Institute of Marine Biological Research of RAS, Sevastopol, Russian Federation; [b]Marine Hydrophysical Institute of RAS, Sevastopol, Russian Federation; [c]Woods Hole Oceanographic Institution, Woods Hole, MA, USA; [d]Institute of Oceanology of Bulgarian Academy of Sciences, Varna, Bulgaria

## ABSTRACT

Bio-optical data, obtained during six cruises in the Black Sea carried out during periods of seasonal stratification in years between 1996 and 2016, have been used to parametrize phytoplankton light absorption ($a_{ph}(\lambda)$) in the deep chlorophyll maximum (DCM) layer located near the bottom of euphotic zone. Relationships between $a_{ph}(\lambda)$ and the sum of chlorophyll-$a$ and phaeopigment concentrations (Chl-$a$) differed from those for the summer-time upper mixed layer (UML). Notably, chlorophyll a specific absorption coefficients ($a_{ph}^*(\lambda)$) were lower in the DCM and more comparable with $a_{ph}^*(\lambda)$ values typical for winter phytoplankton in the Black Sea. The $a_{ph}(\lambda)$ spectral shapes in the DCM differed markedly from those in winter and in the summer UML, due to a shoulder at ~490 nm and a local maximum at ~550 nm corresponding to the absorption bands of phycourobilin and phycoerythrobilin. Light absorbing properties of phytoplankton in the DCM (amplitude and spectral shape of $a_{ph}^*(\lambda)$) reflected physiological acclimation to local conditions on the cellular level and population shifts leading to changes in the biomass-dominant species, with *Synechococcus* spp. domination in the DCM. The parameterization of phytoplankton absorption in the DCM will enable refined spectral models of the downwelling radiance and primary production in the Black Sea.

## Introduction

Remote-sensing (visible spectral radiometric) data are used widely to assess water productivity, and carbon cycle processes (Saba et al., 2011, Behrenfeld et al., 2005) and to study changes caused by environment factors linked to climate and anthropogenic pressures (Behrenfeld et al., 2006). The spectral distribution of water leaving radiance measured by optical scanners (Sea-viewing Wide Field-of-view Sensor (SeaWiFS), Medium Resolution Imaging Spectrometer (MERIS), Moderate Resolution Imaging Spectroradiometer aboard the Terra and Aqua satellites (MODIS-Aqua/Terra)) is influenced by scattering due to particles and water molecules and by absorption due to phytoplankton, non-algal particles (NAP), colored dissolved organic matter (CDOM), and water molecules (Kirk, 2011). To develop algorithms for assessment of productivity indicators based on remote sensing, variability in light absorption coefficient of phytoplankton ($a_{ph}(\lambda)$), NAP ($a_{NAP}(\lambda)$) and CDOM ($a_{CDOM}(\lambda)$) have been studied in the global ocean since the 1980s (Babin et al., 2003; Bricaud, Babin, Morel, & Claustre, 1995; Bricaud, Morel, Babin, Allali, & Claustre, 1998; Cleveland, 1995; Hoepffner & Sathyendranath, 1992;

Sosik & Mitchell, 1995). Inherent optical properties (IOPs) have been shown to vary throughout the world ocean (Babin et al., 2003; Bricaud et al., 1995, 1998). One approach to dealing with this variability is to subdivide the global ocean needs to be subdivided into provinces based on regional IOPs, and then use regional parameterization to improve remote-sensing algorithms for each province (Hoepffner & Sathyendranath, 1992; Lutz et al., 1996, Suzuki, Kishino, Sasaoka, Saitoh, & Saino, 1998).

For the Black Sea, a regional algorithm for retrieval of Chl-$a$ in the surface layer has already been developed (Suslin & Churilova, 2016). Comparison with the other algorithms (Kopelevich, Burenkov, Ershova, Sheberstov, & Evdoshenko, 2004; O'Reilly et al., 2000) showed that the regionally tuned bio-optical algorithm (Suslin & Churilova, 2016) produces Chl-$a$ retrievals with lower error (Suslin et al., 2018). Precise Chl-$a$ assessment is important for downwelling radiance and primary production (PP) algorithms, because they are mostly based on Chl-$a$. Among the algorithms using Chl-$a$ for PP calculation, spectral approaches (Morel, 1991) have significant advantages compared with non-spectral approaches, because they can take into account the

highly variable spectral characteristics of underwater irradiance and phytoplankton absorption (Kirk, 2011).

Development of spectral approach for assessment of primary production in the Black Sea requires assessment of the relationship between $a_{ph}(\lambda)$ and Chl-a. $a_{ph}(\lambda)$ variability in the Black Sea has been studied since 1995 (Berthon, Mélin, & Zibordi, 2008; Chami et al., 2005; Churilova, 2001; Churilova & Berseneva, 2004; Churilova, Berseneva, & Georgieva, 2004; Dmitriev et al., 2009). A dataset collected during several scientific cruises from 2011 to 2015 was used to reveal the relationships between $a_{ph}(\lambda)$ and Chl-a for the upper mixed layer (UML) of the deep water part of the Black Sea in winter and summer (Churilova et al., 2017). To describe the relationship between $a_{ph}(\lambda)$ and Chl-a a power function was used (Bricaud et al., 1995):

$$a_{ph}(\lambda) = A(\lambda) \times (\text{Chl}-a)^{B(\lambda)} \qquad (1)$$

where $A(\lambda)$ is a spectral coefficient, which is equal to $a_{ph}^*(\lambda)$ when Chl-a is equal to 1 mg/m$^3$ and $B(\lambda)$ is a spectral coefficient, which is <1 reflecting a decrease of $a_{ph}^*(\lambda)$ with Chl-a increasing. At blue wavelengths, $A(\lambda)$ differed nearly twofold between summer and winter (Churilova et al., 2017). These significant seasonal differences in $a_{ph}^*(\lambda)$ values were shown to be caused by changes of accessory pigments to chlorophyll-a ratio and intracellular pigment concentration in response to seasonal variability of UML environment conditions mainly light intensity, which differed more than an order of magnitude, because of changes in both incident photosynthetic available radiation (PAR) and the ratio of UML to euphotic zone ($Z_{eu}$) depth (Churilova et al., 2017). Consequently, seasonally different relationships between $a_{ph}(\lambda)$ and Chl-a are required for correct assessment of downwelling radiance and primary production in the Black Sea with spectral approaches. To date, however, no studies have investigated variability in the $a_{ph}(\lambda)$ and Chl-a relationship below the UML during summertime. This is important because the summertime UML in deep- and shelf waters (not in shallow coastal) is shallower than $Z_{eu}$ (Churilova et al., 2017; Vedernikov, 1989). Seasonal water stratification (maximum temperature gradient, TC) divides $Z_{eu}$ into quasi-isolated layers: the UML and a layer below TC (BTC). These layers differ in environmental conditions, namely temperature (Ivanov & Belokopytov, 2011), nutrient availability (Krivenko & Parkhomenko, 2015), and intensity and spectral composition of irradiance (Kopelevich, Sheberstov, Burenkov, Vazyulya, & Likhacheva, 2007; Vazyulya & Sheberstov, 2017). In stratified waters, the Chl-a vertical profile typically has a deep chlorophyll maximum (DCM) (Finenko, Churilova, & Lee, 2005; Vedernikov, 1989; Yunev, Moncheva, & Carstensen, 2005) located near the bottom of $Z_{eu}$ (~1%PAR) (Finenko et al., 2005). Phytoplankton assemblages in the BTC differed from those in the UML in terms of species composition and intracellular pigment concentration (Finenko et al., 2005; Georgieva, 1993; Rat'kova, 1989, Senichkina, Georgieva, Nesterova, Fashchuk, & Lifshiz, 1991). Theoretical studies (Morel & Bricaud, 1981), quantitative experiments with microalgae cultures (Fujiki & Taguchi, 2002; Sosik & Mitchell, 1991, 1994) and our previous results obtained for UML of the Black Sea (Churilova et al., 2017) showed dependence of $a_{ph}^*(\lambda)$ on pigment composition and concentration in the algae cells. Consequently, deep phytoplankton assemblages are expected to differ from those in the UML, which in turn suggests that $a_{ph}^*(\lambda)$, and therefore the coefficients ($A(\lambda)$ and $B(\lambda)$) of phytoplankton absorption parametrization, will differ in the DCM.

The aim of the current research is to analyze variability of phytoplankton light absorption coefficients in the DCM layer during warm periods of the year, when water is seasonally stratified in the Black Sea, and specifically to parameterize the relationship between the phytoplankton absorption coefficient and chlorophyll-a concentration.

## Materials and methods

### Water sampling

For this research we combined bio-optical data obtained in seasonally stratified waters, when the UML was shallower than $Z_{eu}$, determined as the depth where PAR is attenuated to 1% of the surface value. We compiled a dataset that includes observations in deep and continental shelf regions of the Black Sea (excluding coastal areas <50 m), where water column structure is influenced by the balance of solar heating and wind generated mixing. The data were collected in different regions of the Black Sea on six cruises during years between 1996 and 2016 (Table 1, Figure 1).

A SBE-911plus (Sea Bird Electronics; for Tr16, VP, PV79, PV85 cruises) or MARK-III (Neil Brown

Table 1. Information about scientific cruises in the Black Sea.

| Cruise | Year | Date | Investigation area of the Black Sea |
|---|---|---|---|
| Tr16 | 1996 | 7–22 June | Deep and shelf western region |
| VP | 2005 | 20 September–15 October | Deep and shelf western region |
| PV69 | 2011 | 2–11 August | Deep western region |
| PV70 | 2011 | 19–27 August | Deep western region |
| PV79 | 2015 | 25–30 September | Deep eastern region |
| PV85 | 2016 | 26–30 May | Deep western and eastern region |

Comments: Tr – RV "Trepang", VP – RV "Vladimir Parshin", PV – RV "Professor Vodyanitsky".
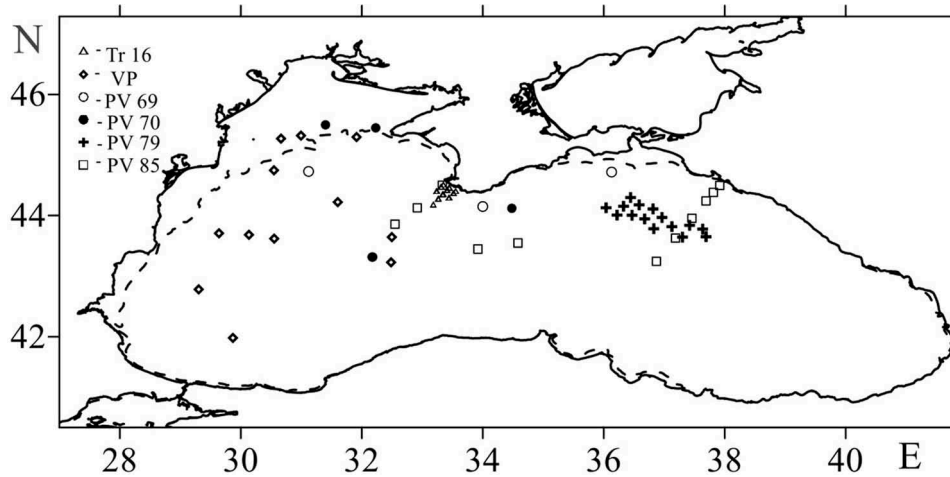
**Figure 1.**

Ocean Sensors, Inc.; for PV69 and PV70 cruises) conductivity, temperature, depth (CTD) probe provided profiles of temperature and salinity, and the rosette included 12 × 5-liter Niskin bottles for water collection. On the Tr16, VP, and PV85 cruises, a chlorophyll fluorometer was integrated with the CTD probe, and a PAR sensor was also added on Tr16 and VP. Water samples were collected on the upcast of the CTD deployment with sample depths chosen on the basis of the real-time fluorescence, temperature, and PAR profiles on all cruises except for PV69 and PV70, where sampling depths were chosen from temperature profiles and water transparency assessed by Secchi disk depth ($Z_s$). On the PV69 and PV70 cruises, *in situ* irradiance (1% and 0.1% of PAR at the sea surface) was assessed from $Z_s$ as described in Churilova et al. (2017).

### Pigment analysis

Samples for pigment and particulate light absorption analysis were gently vacuum (<25 kPa) filtered through 25-mm Whatman GF/F filters and stored in liquid nitrogen for return to the laboratory. Filters were extracted overnight in cold 90% acetone, then were treated with a vibration mixer (FALK Falc instruments, Italy) and centrifuged. Chlorophyll and phaeopigment concentrations were determined spectrophotometrically (Jeffry & Humphry, 1975; Lorenzen, 1967) on the PV79 and PV85 cruises, with a dual-beam spectrophotometer (Lambda 35; Perkin Elmer) and fluorometrically (Holm-Hansen, Lorenzen, Holmes, & Strickland, 1965) on the Tr16, VP, PV69, and PV70 cruises, with a fluorometer calibrated with pure chlorophyll-a. Comparison of the fluorometer and spectrophotometer results showed that they were in good agreement and can be used for joint analysis.

### Light absorption by phytoplankton

The sample processing for phytoplankton absorption followed recommended ocean optics protocols (Mitchell, Kahru, Wieland, & Stramska, 2003). Particulate light absorption was determined by the filter pad technique ("wet filter technique") (Mitchell & Kiefer, 1988; Yentsch, 1962). Phytoplankton light absorption ($a_{ph}(\lambda)$) was calculated by the difference between total particulate matter absorption ($a_p(\lambda)$) and $a_{NAP}(\lambda)$ :

$$a_{ph}(\lambda) = a_p(\lambda) - a_{NAP}(\lambda) \qquad (2)$$

Values of $a_{ph}(\lambda)$ were calculated from measured optical densities after correction for scattering (setting the mean absorption between 720 and 750 nm to zero) and for the path length amplification factor applying the quadratic equation described by Mitchell (1990). Optical measurements of the absorption coefficient of particles were made over the spectral region from 350 to 750 nm with a dual-beam spectrophotometer (SPECORD – M40, Carl Zeis Yena) (Tr16, VP, PV69 and PV70 cruises) or with a dual-beam spectrophotometer (Lambda 35, Perkin Elmer) equipped with a Spectralon integrating sphere (PV79, PV85). $a_{NAP}(\lambda)$ values were determined for samples collected during the Tr16 and VP cruises using pigment extraction with methanol (Kishino, Takahashi, Okami, & Ichimura, 1985). After methanol treatment, some $a_{NAP}(\lambda)$ spectra (in particular from depths near the bottom of the euphotic zone) had optical traces of remaining phycobillins at ~550 nm (Figure 2). To estimate $a_{ph}(\lambda)$ including absorption by all pigments, we had to correct the $a_{NAP}(\lambda)$ spectra. For this aim $a_{NAP}(\lambda)$ spectra were represented as exponential functions (Babin et al., 2003):

$$a_{NAP}(\lambda) = a_{NAP}(\lambda_r)e^{(-S_{NAP}(\lambda-\lambda_r))} \qquad (3)$$

where $\lambda_r$ is a reference wavelength (in this research $\lambda_r$ = 440 nm), and $S_{NAP}$ is the spectral slope. The fit
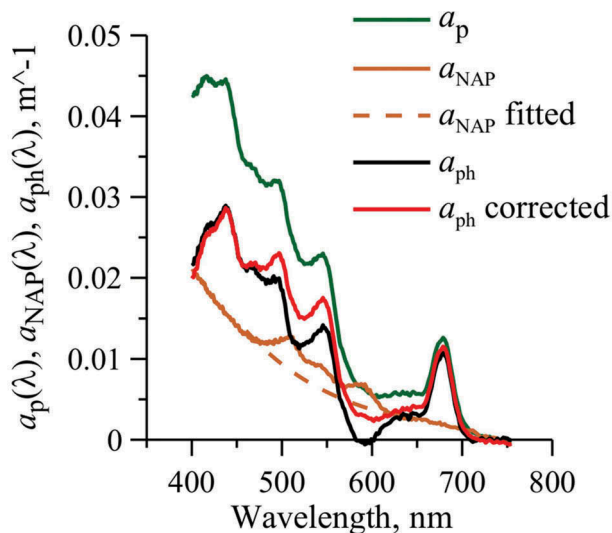
**Figure 2.** Example (st.30, 50 m, 2005) of light absorption spectra for total particles ($a_p(\lambda)$, green line); non-algal particles ($a_{NAP}(\lambda)$), brown line, dashed brown line for exponential fit); and phytoplankton $a_{ph}(\lambda)$, black and red lines respectively indicating before and after correction with the $a_{NAP}(\lambda)$ exponential fit.

was done for data between 400 and 700 nm, excluding the 490–610 nm ranges to avoid residual pigment absorption (Figure 2). For the samples collected on the PV69, PV70, PV79, and PV85 cruises, $a_{NAP}(\lambda)$ was determined after pigment bleaching with sodium hypochlorite (Tassan & Ferrari, 1995). To compute Chl-$a$ specific light absorption coefficients of phytoplankton ($a_{ph}^*(\lambda)$) (m$^2$/mg), the values of $a_{ph}(\lambda)$ (m$^{-1}$) were divided by the sum of chlorophyll-$a$ and phaeopigments concentrations (Chl-$a$) (mg/m$^3$). Relationships between $a_{ph}(\lambda)$ and Chl-$a$ were derived by least squares fitting to power functions for the visible spectral domain 400–700 nm with 1-nm resolution.

### Phytoplankton

Samples were concentrated with a reverse filtration system through 1 μm nucleopore filters, and then stored in buffered formaldehyde (2.5% final concentration). Counting of phytoplankton cells and identification of phytoplankton species (micro- and nano-size fractions) were performed in a Naumann chamber with a transmission microscope (Ergaval; Carl Zeiss Jena). Cells were sized and cell volumes were assessed using geometrical figures (sphere, ellipsoid or cylinder) corresponding to the cell shapes. The phytoplankton (micro- and nano-fractions) were analyzed on samples from the Tr16 and VP cruises. On these cruises, phototrophic picoplankton cell number and size were estimated by the method of MacIsaac and Stockner (1993). Samples were preserved with paraformaldehyde, then filtered onto 0.2 μm nucleopore filters («Nucleopore» USA) and stored in liquid

nitrogen before analysis in the laboratory. The picoplankton cells were counted on a Carl Zeiss Jenalumar epifluorescent microscope.

On the PV69, PV70, PV79 and PV85 cruises, picoplankton were analyzed by flow cytometry. Samples were preserved in paraformaldehyde to a final concentration of 2%, then frozen in liquid nitrogen (−80°C) and stored at −20°C before analysis in the laboratory. Analysis was carried out with a Cytomics FC 500 (Beckman Coulter, USA) flow cytometer equipped with a single-phase argon laser (488 nm) (Marie, Partensky, Vaulot, & Brussaard, 1999; Schapira, Buscot, Pollet, Leterme, & Seuront, 2010). For all detected particles, phycoerythrin fluorescence emission (575 nm) and chlorophyll fluorescence emission (675 nm) were measured. The flow cytometer measurements were calibrated with the Fluorospheres Flow-CheckTM (Beckman Coulter). Cytometric data were analyzed using CXP software (Beckman Coulter).

## Results

### Chlorophyll-a concentration

In June 1996 in the investigated area (Figure 1), the UML was shallow (7–12 m) (Figure 3). $Z_{eu}$ varied from 28 to 38 m. The vertical distribution of chlorophyll fluorescence (Flu) showed a DCM located near the 1% PAR level. Deeper secondary maxima (smaller peaks in Flu) in the 40–60 m water layer were detected at most stations. In the DCM layer Chl-$a$ values (0.60–1.40 mg/m$^3$) were 4–7-fold higher than UML Chl-$a$ values (0.15–0.44 mg/m$^3$).

During the period 25 September–15 October 2005, seasonal water stratification persisted in deep- and shelf water regions (Figure 3). The UML was deepened to 14–22 m, but did not reach the bottom of $Z_{eu}$, which varied from 35 to 48 m (Table 1). In October 2005, hydrographic characteristics of the water column corresponded to the summer-type conditions, with a narrow layer of thermocline (4–7 m) and a high temperature gradient (1.4–7.0°C/m), which was fixed at 15–23 m. In the UML, the Chl-$a$ distribution was almost uniform. The surface Chl-$a$ ranged from 0.33 to 0.85 mg/m$^3$. The DCM was located below the layer of maximum temperature gradient and near the 1% PAR depth. In the DCM, Chl-$a$ values were ~3–4 times higher than UML concentrations.

In the western part of the Black Sea during August 2011, a seasonal thermocline was well developed, with maximum temperature gradient reaching ~6°C/m and UML −7 to 11 m (Figure 3). In August, $Z_{eu}$ varied between 30 and 46 m. The vertical Chl-$a$ profile was characterized by a rather homogeneous distribution within the UML and a DCM located near
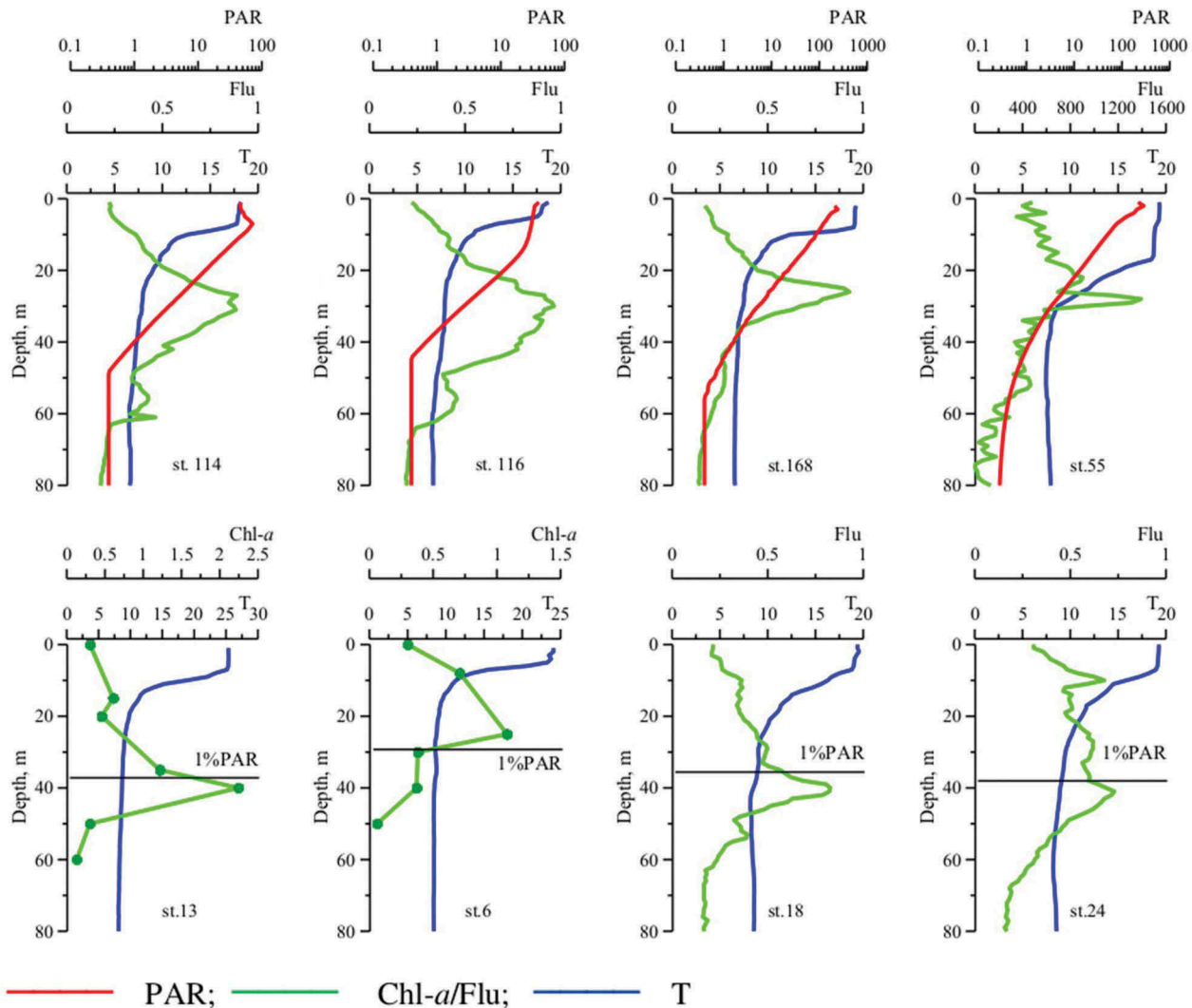
**Figure 3.** Example vertical profiles of temperature (T, oC, blue line), chlorophyll a fluorescence (Flu, rel. units, green), concentration of chlorophyll-a plus phaeopigments (Chl-*a*, mg/m³, circles), photosynthetically available radiation (PAR, mE/m²/s, red line) in the Black Sea at different times (st. 114, 19 June 1996; st. 116, 19 June 1996; st. 168, 22 June 1996; st. 55, 14 October 2005; st. 13,-21 August 2011; st. 6, 27 September 2015; st. 18, 28 May 2016; st. 24, 28 May 2016).

the bottom of $Z_{eu}$. Values of Chl-*a* in the DCM layer (0.87 to 2.4 mg/m³) were 5–10 times higher than in the UML (0.15–0.30 mg/m³).

In September 2015 in the eastern part of the Black Sea (Figure 1), hydrographic structure was similar to that in summer, with typical high temperature gradients (4.3 ± 1.2°C/m) and UML –6 to 12 m (Figure 3). $Z_{eu}$ varied from 30 to 45m, depths that exceeded the UML thickness by 3–5-fold. In the sea surface layer, Chl-*a* values (0.21–0.35 mg/m³) were comparable with those measured in summer (June 1996, August 2011). Vertical Chl-*a* distribution was similar to that observed in summer: a DCM was detected near the bottom of $Z_{eu}$ (Figure 3). In the DCM layer, Chl-*a* values (0.61–1.72 mg/m³) were 3–6 times higher than in the UML.

At the end of May 2016 in the deep waters (Figure 1), the UML did not exceed 10 m, while the thermocline spread within a ~10–40 m layer with weak (in comparison with summer) maximal

temperature gradient (0.06–1.3°C/m) located between 10 and 15 m (Figure 3). Flu profiles showed a DCM in the 35–50 m layer. The DCM was located in general near the bottom of both the thermocline and $Z_{eu}$. Below the DCM, small Flu maxima were detected at several stations. In the thermocline at depths of maximal temperature (density) gradients, local Flu peaks were observed. Chl-*a* varied from 0.31 to 0.64 mg/m³ in the surface layer and from 0.81 to 1.4 mg/m³ in the DCM layer.

## Light absorption by phytoplankton

On all cruises light absorption coefficients and spectra shape changed markedly within water column (Figure 4). For all $a_{ph}(\lambda)$ spectra, two main peaks were typical: in the blue (near 440 nm) and red (near 678 nm) spectral domains. In the UML, the ratio between blue and red peaks (R) was in a range
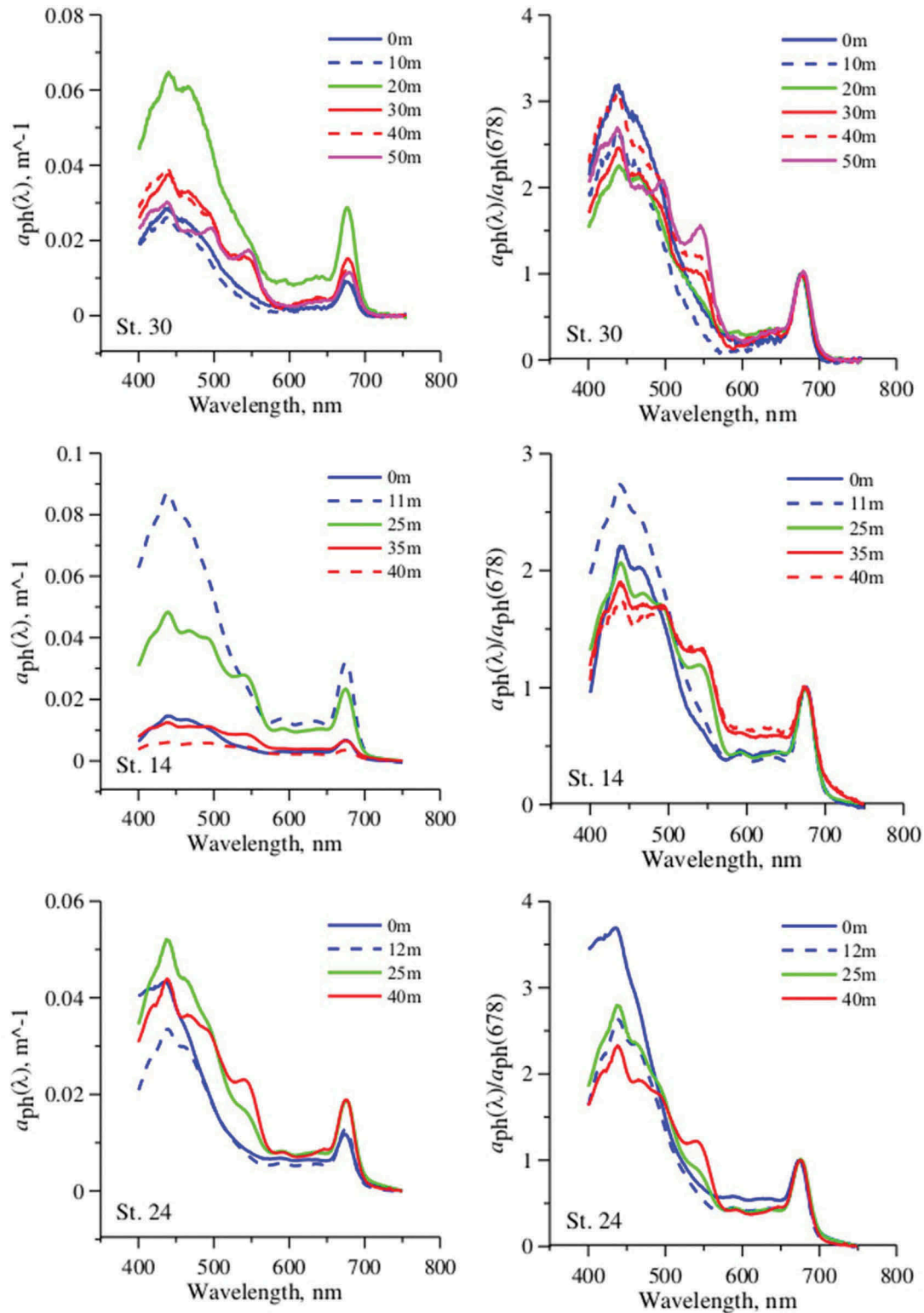
**Figure 4.** Phytoplankton light absorption spectra ($a_{ph}(\lambda)$) and ($a_{ph}(\lambda)$) normalized at 678 nm ($a_{ph}(\lambda)/a_{ph}(678)$), obtained at different depths in October 2005 (st. 30), in September 2015 (st. 14), and in May 2016 (st. 24).

3.2–4.1 (June 1996, May 2016), 2.7–3.8 (August 2011), 2.2–3.6 (September 2015) and 2.3–3.1 (October 2005). In the BTC layer, $a_{ph}(\lambda)$ shapes differed from those in the UML, with lower R (1.7–3.1) and appearance of a shoulder at ~490 nm and local maximum at ~550 nm, which became more pronounced with depth (Figure 4).

The bio-optical dataset for the BTC layer represents the DCM layer because this dataset generally includes data from the DCM layer data and only a few samples from the small Chl-a peak below the DCM (Figure 3). $a_{ph}(\lambda)$ at blue (~440 nm) and red (678 nm) peaks co-varied with Chl-a, with the relationship well described by a power function

**Figure 5.** Dependence of phytoplankton light absorption coefficients at red $(a_{ph}(678))$ (A) and blue $(a_{ph}(440))$ (B) peaks on the sum of chlorophyll-a and phaeopigment concentrations (Chl-a) in the deep ch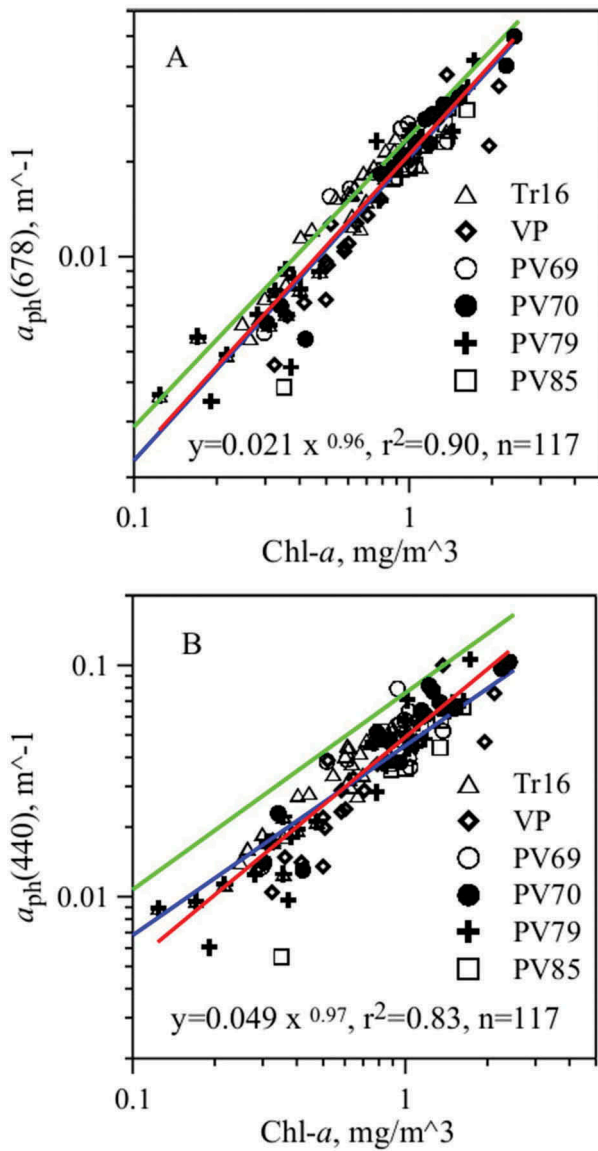lorophyll maximum (DCM) layer in the Black Sea during June 1996 (Tr16, triangles), October 2005 (VP, diamonds), August 2011 (PV69, circles, PV70, filled circles), September 2015 (PV79, crosses), and May 2016 (PV85, squares). Red lines denote the power function fit to these data (Eqns. 4 and 5). Green and blue lines show fits obtained for the upper mixed layer in summer and winter from Churilova et al. [2017].

(Equation 1) (Figure 5) (near here). For the DCM layer, the following fit equations were obtained:

$$a_{ph}(440) = 0.049 \times (Chl-a)^{0.97} \left( r^2 = 0.83 \right) \quad (4)$$

$$a_{ph}(678) = 0.021 \times (Chl-a)^{0.96} \left( r^2 = 0.90 \right) \quad (5)$$

The dependence of $a_{ph}(678)$ and $a_{ph}(440)$ on Chl-a were close to those obtained for the UML in the Black Sea in winter (Churilova et al., 2017) and those revealed based on numerous data measured in different regions of the global ocean (Bricaud et al., 1995). However, the relationships for the DCM differed

from those for the UML of the Black Sea in summer, with lower values of $a_{ph}(\lambda)$ for a given Chl-a. This difference was more pronounced for $a_{ph}(440)$ values compared to $a_{ph}(678)$.

To retrieve the $a_{ph}(\lambda)$ spectrum based on Chl-a, relationships need to be determined for the entire visible spectrum from 400 to 700 nm with high spectral resolution. The $a_{ph}(\lambda)$ vs Chl-a dependence was parameterized using Equation (1). The results of this parameterization provide coefficients for the visible domain with 2 nm spectral resolution (Table 2 and Figure 6). Throughout the visible range, A($\lambda$) coefficients for the DCM are comparable with coefficients found for the winter UML in the Black Sea (Churilova et al., 2017) and agreed with results of parameterization of the light absorption by phytoplankton in the global ocean (Bricaud et al., 1995). In contrast, A($\lambda$) coefficients are about twofold lower in the blue domain for the DCM compared to the UML in summer in the Black Sea. An even more crucial difference in the shape of A($\lambda$) is related to the local maximum at ~550 nm (Figure 6).

### Phytoplankton

Vertical distributions of total biomass of phytoplankton ($B_{tot}$), abundance of cyanobacteria (*Synechococcus* spp) ($N_{pico}$), contribution of *Synechococcus* spp to $B_{tot}$ ($B_{pico}$) were determined in the western deep and shelf waters of the Black Sea in June 1996 and in October 2005 (Figure 7). In June 1996, values of $B_{tot}$ were in a range from 9 to 200 mg/m$^3$ without an evident maximum at the DCM. Phytoplankton analysis showed that in June the UML biomass of phytoplankton (nano- and micro fraction) was generally composed of two classes: Dinophyceae and Prymnesiophyceae, which contributed 60% (±15) and 23% (±17) to the total biomass, respectively. In the DCM layer, the phytoplankton was dominated (in biomass) by *Dinophyceae* (77 ± 14%). To estimate the ratio between organic carbon and chlorophyll-a concentration (C/Chl), the C content was estimated as 10% of the "wet" weight of phytoplankton. In the DCM layer, C/Chl was ~5–26 mg/mg. In the UML layer (0–10 m), cyanobacteria were abundant ((2.3–22) × 10$^9$ cell/m$^3$) and accounted for 95% or more of the total number of phototrophic picoplankton. Below the UML, $N_{pico}$ generally varied from 1.6 × 10$^9$ to 60 × 10$^9$ cell/m$^3$, with the exception of two points with high values (82 and 190) × 10$^9$ cell/m$^3$). $N_{pico}$ profiles showed a tendency to increase at 50–60 m depths (Figure 7). The contribution of cyanobacteria to total phytoplankton biomass was 1.4–5.5% in the UML and increased in deeper waters, reaching ~60% at 50–60 m depths.

In early October 2005 in deep western waters, $B_{tot}$ generally varied over the water column (0–50 m)

**Table 2.** Spectral values of the constants obtained when fitting variations of $a_{ph}(\lambda)$ versus the chlorophyll-a plus phaeopigment concentrations (Chl-a) to power laws of the form $a_{ph}(\lambda) = A(\lambda) \times (\text{Chl}-a)^{B(\lambda)}$, and standard deviations (SD) calculated on the log-transformed data.

| λ | A(λ) | SD | B(λ) | λ | A(λ) | SD | B(λ) |
|---|------|-----|------|---|------|-----|------|
| 400 | 0.0312 | 0.3107 | 0.9193 | 472 | 0.0388 | 0.2491 | 0.9835 |
| 402 | 0.0320 | 0.3037 | 0.9174 | 474 | 0.0382 | 0.2469 | 0.9825 |
| 404 | 0.0330 | 0.2948 | 0.9268 | 476 | 0.0376 | 0.2431 | 0.9800 |
| 406 | 0.0341 | 0.2880 | 0.9283 | 478 | 0.0370 | 0.2435 | 0.9804 |
| 408 | 0.0353 | 0.2821 | 0.9313 | 480 | 0.0364 | 0.2432 | 0.9776 |
| 410 | 0.0365 | 0.2767 | 0.9362 | 482 | 0.0358 | 0.2415 | 0.9771 |
| 412 | 0.0376 | 0.2758 | 0.9371 | 484 | 0.0354 | 0.2434 | 0.9765 |
| 414 | 0.0386 | 0.2732 | 0.9380 | 486 | 0.0349 | 0.2441 | 0.9738 |
| 416 | 0.0394 | 0.2721 | 0.9393 | 488 | 0.0345 | 0.2455 | 0.9713 |
| 418 | 0.0399 | 0.2728 | 0.9412 | 490 | 0.0341 | 0.2469 | 0.9688 |
| 420 | 0.0404 | 0.2724 | 0.9419 | 492 | 0.0335 | 0.2508 | 0.9677 |
| 422 | 0.0408 | 0.2727 | 0.9462 | 494 | 0.0329 | 0.2532 | 0.9682 |
| 424 | 0.0412 | 0.2723 | 0.9502 | 496 | 0.0323 | 0.2564 | 0.9670 |
| 426 | 0.0418 | 0.2722 | 0.9543 | 498 | 0.0314 | 0.2568 | 0.9644 |
| 428 | 0.0426 | 0.2720 | 0.9584 | 500 | 0.0304 | 0.2575 | 0.9689 |
| 430 | 0.0435 | 0.2707 | 0.9653 | 502 | 0.0292 | 0.2595 | 0.9727 |
| 432 | 0.0444 | 0.2713 | 0.9712 | 504 | 0.0280 | 0.2592 | 0.9733 |
| 434 | 0.0454 | 0.2704 | 0.9744 | 506 | 0.0269 | 0.2582 | 0.9819 |
| 436 | 0.0461 | 0.2714 | 0.9771 | 508 | 0.0258 | 0.2560 | 0.9880 |
| 438 | 0.0464 | 0.2711 | 0.9802 | 510 | 0.0248 | 0.2549 | 0.9886 |
| 440 | 0.0463 | 0.2718 | 0.9786 | 512 | 0.0239 | 0.2568 | 0.9924 |
| 442 | 0.0457 | 0.2727 | 0.9804 | 514 | 0.0233 | 0.2523 | 0.9932 |
| 444 | 0.0449 | 0.2729 | 0.9813 | 516 | 0.0226 | 0.2537 | 0.9906 |
| 446 | 0.0438 | 0.2714 | 0.9816 | 518 | 0.0221 | 0.2527 | 0.9878 |
| 448 | 0.0426 | 0.2706 | 0.9828 | 520 | 0.0216 | 0.2529 | 0.9843 |
| 450 | 0.0415 | 0.2693 | 0.9831 | 522 | 0.0211 | 0.2572 | 0.9829 |
| 452 | 0.0406 | 0.2686 | 0.9870 | 524 | 0.0208 | 0.2590 | 0.9740 |
| 454 | 0.0400 | 0.2683 | 0.9892 | 526 | 0.0205 | 0.2643 | 0.9701 |
| 456 | 0.0397 | 0.2673 | 0.9882 | 528 | 0.0203 | 0.2650 | 0.9670 |
| 458 | 0.0395 | 0.2667 | 0.9902 | 530 | 0.0201 | 0.2695 | 0.9580 |
| 460 | 0.0396 | 0.2646 | 0.9924 | 532 | 0.0200 | 0.2728 | 0.9559 |
| 462 | 0.0397 | 0.2626 | 0.9939 | 534 | 0.0198 | 0.2810 | 0.9537 |
| 464 | 0.0397 | 0.2592 | 0.9917 | 536 | 0.0197 | 0.2845 | 0.9505 |
| 466 | 0.0397 | 0.2558 | 0.9908 | 538 | 0.0196 | 0.2939 | 0.9459 |
| 468 | 0.0396 | 0.2543 | 0.9875 | 540 | 0.0194 | 0.2984 | 0.9392 |
| 470 | 0.0392 | 0.2506 | 0.9836 | 542 | 0.0192 | 0.3020 | 0.9342 |

| λ | A | SD | B | λ | A | SD | B |
|---|------|-----|------|---|------|-----|------|
| 544 | 0.0189 | 0.3092 | 0.9287 | 626 | 0.0070 | 0.2894 | 0.9200 |
| 546 | 0.0184 | 0.3169 | 0.9302 | 628 | 0.0070 | 0.2916 | 0.9237 |
| 548 | 0.0179 | 0.3196 | 0.9263 | 630 | 0.0071 | 0.2772 | 0.9221 |
| 550 | 0.0173 | 0.3227 | 0.9232 | 632 | 0.0073 | 0.2672 | 0.9172 |
| 552 | 0.0164 | 0.3258 | 0.9212 | 634 | 0.0074 | 0.2616 | 1.0144 |
| 554 | 0.0155 | 0.3274 | 0.9237 | 636 | 0.0076 | 0.2456 | 1.0048 |
| 556 | 0.0143 | 0.3281 | 0.9272 | 638 | 0.0078 | 0.2321 | 1.0010 |
| 558 | 0.0132 | 0.3316 | 0.9424 | 640 | 0.0078 | 0.2330 | 1.0060 |
| 560 | 0.0120 | 0.3354 | 0.9411 | 642 | 0.0079 | 0.2339 | 1.0087 |
| 562 | 0.0109 | 0.3338 | 0.9600 | 644 | 0.0079 | 0.2231 | 0.9835 |
| 564 | 0.0099 | 0.3268 | 0.9669 | 646 | 0.0080 | 0.2157 | 0.9767 |
| 566 | 0.0091 | 0.3389 | 0.9807 | 648 | 0.0079 | 0.2179 | 0.9664 |
| 568 | 0.0084 | 0.3441 | 1.0416 | 650 | 0.0079 | 0.2218 | 0.9494 |
| 570 | 0.0078 | 0.3475 | 1.0273 | 652 | 0.0079 | 0.2168 | 0.9567 |
| 572 | 0.0074 | 0.3596 | 1.0360 | 654 | 0.0081 | 0.2135 | 0.9441 |
| 574 | 0.0070 | 0.3736 | 1.0978 | 656 | 0.0084 | 0.2189 | 0.9637 |
| 576 | 0.0066 | 0.4095 | 1.0203 | 658 | 0.0090 | 0.2154 | 0.9651 |
| 578 | 0.0064 | 0.4127 | 1.0390 | 660 | 0.0099 | 0.2091 | 0.9582 |
| 580 | 0.0062 | 0.4181 | 1.1525 | 662 | 0.0111 | 0.2070 | 0.9614 |
| 582 | 0.0061 | 0.4429 | 1.0979 | 664 | 0.0127 | 0.1978 | 0.9644 |
| 584 | 0.0060 | 0.4743 | 1.0714 | 666 | 0.0145 | 0.1901 | 0.9724 |
| 586 | 0.0060 | 0.4852 | 0.9893 | 668 | 0.0163 | 0.1836 | 0.9724 |
| 588 | 0.0059 | 0.5113 | 0.9866 | 670 | 0.0179 | 0.1787 | 0.9706 |
| 590 | 0.0059 | 0.5407 | 1.0646 | 672 | 0.0192 | 0.1752 | 0.9746 |
| 592 | 0.0059 | 0.5546 | 0.9974 | 674 | 0.0200 | 0.1755 | 0.9747 |
| 594 | 0.0059 | 0.5173 | 0.9804 | 676 | 0.0203 | 0.1763 | 0.9654 |
| 596 | 0.0060 | 0.4677 | 1.0167 | 678 | 0.0200 | 0.1802 | 0.9619 |
| 598 | 0.0059 | 0.4488 | 1.0854 | 680 | 0.0192 | 0.1866 | 0.9526 |
| 600 | 0.0057 | 0.4677 | 1.0883 | 682 | 0.0178 | 0.1940 | 0.9394 |
| 602 | 0.0057 | 0.4592 | 1.0985 | 684 | 0.0158 | 0.2063 | 0.9358 |
| 604 | 0.0057 | 0.4507 | 1.0545 | 686 | 0.0136 | 0.2177 | 0.9238 |
| 606 | 0.0057 | 0.4318 | 1.0177 | 688 | 0.0113 | 0.2277 | 0.9152 |
| 608 | 0.0058 | 0.3880 | 0.9660 | 690 | 0.0091 | 0.2401 | 0.9156 |
| 610 | 0.0059 | 0.3667 | 0.9452 | 692 | 0.0073 | 0.2447 | 0.9184 |
| 612 | 0.0059 | 0.3986 | 0.9803 | 694 | 0.0057 | 0.2537 | 0.9357 |

(Continued)

**Table 2.** (Continued).

| λ | A(λ) | SD | B(λ) | λ | A(λ) | SD | B(λ) |
|---|------|-----|------|---|------|-----|------|
| 614 | 0.0061 | 0.4110 | 0.9804 | 696 | 0.0044 | 0.2782 | 0.9501 |
| 616 | 0.0063 | 0.3553 | 0.9341 | 698 | 0.0034 | 0.2964 | 0.9126 |
| 618 | 0.0065 | 0.3253 | 0.9175 | 700 | 0.0026 | 0.3348 | 0.9047 |
| 620 | 0.0066 | 0.3181 | 0.9239 | | | | |
| 622 | 0.0067 | 0.3084 | 0.9200 | | | | |
| 624 | 0.0068 | 0.3002 | 0.9089 | | | | |

from 66 to 2050 mg/m³, with the exception of one point with high $B_{tot}$ (4800 mg/m³) (Figure 7). The phytoplankton biomass within the euphotic zone was mainly accounted by Bacillariophyceae species (especially *Pseudosolenia calcar-avis* and *Proboscia alata*). In the DCM layer, the C/Chl ratio was ~10–28 mg/mg. *Synechococcus* abundance in the UML was (2–48) × 10⁹ cells/m³ and increased to (9–82) × 10⁹ cells/m³ in the DCM layer. The contribution of cyanobacteria to total biomass increased from 1.1% to 3.8% in the UML and from 32% to 50% in the DCM.

During August 2011 in the deep western waters, $B_{tot}$ in the UML was in the range 66–590 mg/m³. At station 13 (Figure 3), phytoplankton biomass was assessed at several depths within 0–60 m. The result showed a decrease of $B_{tot}$ with increasing depth from 550 mg/m³ to 31 mg/m³. The C/Chl ratio decreased with depth from 180 mg/mg in the surface to 4–24 mg/mg in the 40–60 m layer. The phytoplankton was dominated by Dinophyceae.

Vertical profiles of $N_{pico}$ were determined in August 2011, September 2015 and May 2016 with flow cytometry (Figure 8,). $N_{pico}$ varied from 0.1 to 62 × 10⁹ cell/m³ in August 2011, from 0.2 to 69 × 10⁹ cell/m³ in September 2015 and from 0.02 to 11 × 10⁹ cell/m³ in May 2016. The vertical profiles of $N_{pico}$ in August 2011, in September 2015 and in May 2016 showed a maximum at 30–50 m depths.

## Discussion

Species composition of phytoplankton and its functional characteristics (including light absorbance capacity) depend on acclimation and adaptation of phytoplankton assemblages to ambient environmental conditions. Water column structure is strongly influenced by solar heating. As a result, in warm periods of the year, the upper water layer is stratified. Phytoplankton in DCM layer changes its structural and functional characteristics in response to lower temperature, higher nutrient availability and specific light conditions in comparison with the UML. Underwater light changes with depth both in quantity, and quality. Measurements of the downwelling radiance spectrum carried out in the Black Sea in May 2016 (Vazyulya & Sheberstov, 2017), as well as
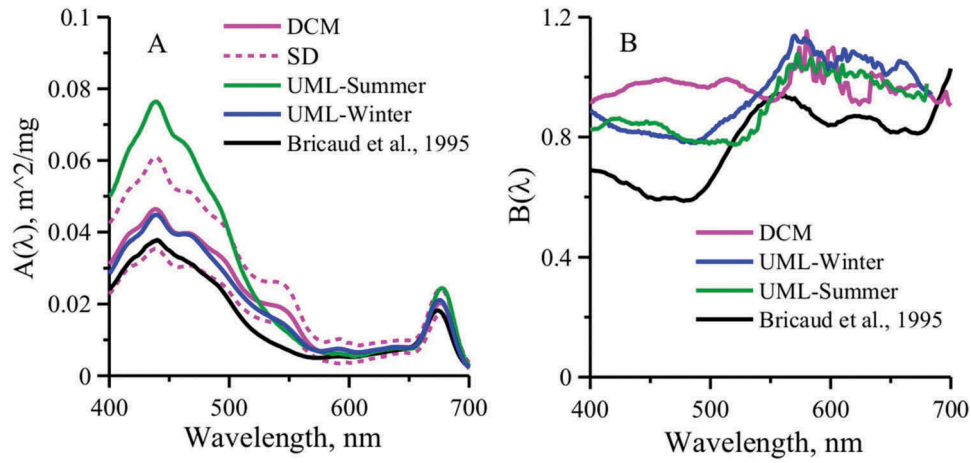
**Figure 6.** Spectral values of the constants $A(\lambda)$ (A) and $B(\lambda)$ (B) obtained when fitting power laws of the form $a_{ph}(\lambda) = A(\lambda)$ (Chl-$a)^{(\lambda)}$ to the variations of phytoplankton light absorption ($a_{ph}(\lambda)$) versus the sum of chlorophyll-$a$ and phaeopigment concentrations (Chl-$a$) for the deep chlorophyll maximum (DCM) layer in the Black Sea (pink lines, dotted lines -SD). Comparison data are shown for the upper mixed layer (UML) in summer (green lines) and in winter (blue lines) according to Churilova et al. [2017] and for a global data set (black lines) described by Bricaud et al. [1995].
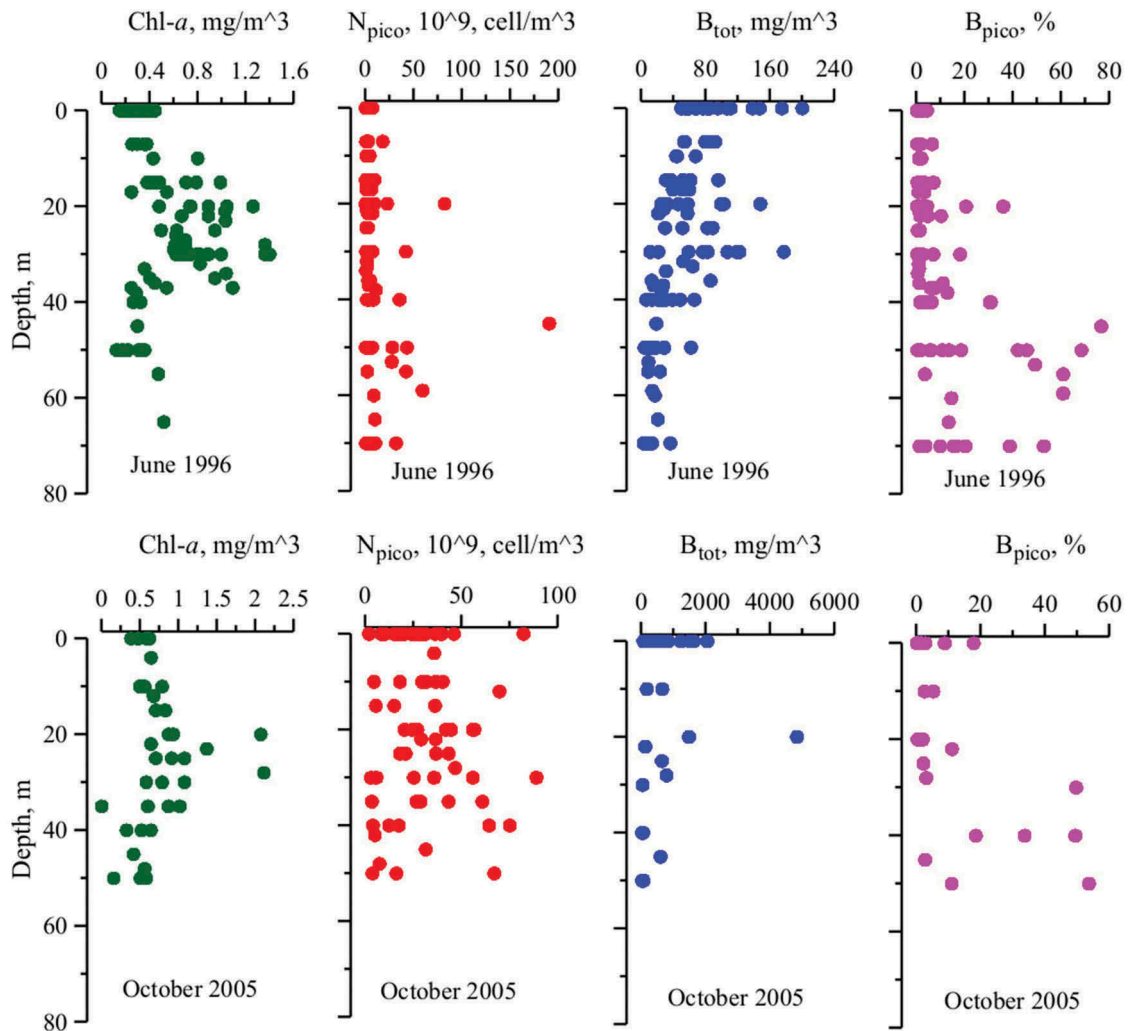


**Figure 7.** Vertical distribution of chlorophyll-a plus phaeopigment concentration (Chl-$a$, mg/m³, green), abundance of cyanobacteria ($N_{pico}$ 10⁹, cell/m³, red), total biomass ("wet") of phytoplankton ($B_{tot}$, mg/m³, blue), cyanobacteria contribution to total biomass ($B_{pico}$, %, pink) in the western part of the Black Sea in June 1996 and in October 2005.

modelling of light attenuation (Churilova, Suslin, & Sosik, 2009; Kopelevich et al., 2007) showed that blue green light (490–590 nm) penetrates preferentially to the bottom of the euphotic layer.
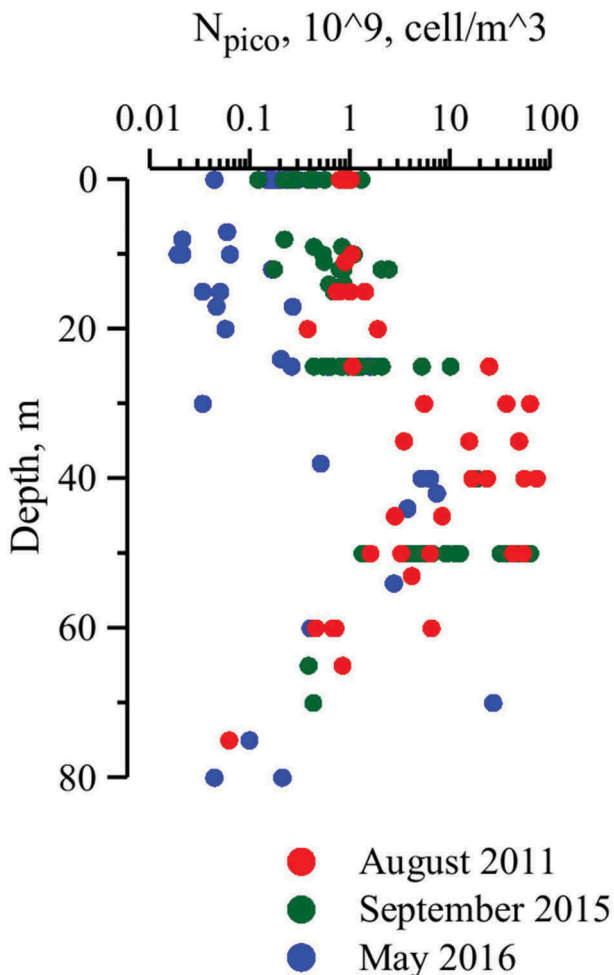
**Figure 8.** Vertical distribution of picocyanobacteria (*Synechococcus* spp) cell concentration ($N_{pico}$) in deep waters of the Black Sea in August 2011 (red), in September 2015 (green) and in May 2016 (blue), obtained from analytical flow cytometry.

Light absorbance properties of the phytoplankton are sensitive to the water environment and change as the phytoplankton acclimates. Relationships between $a_{ph}(440)/a_{ph}(678)$ and Chl-*a* (Figure 5) in the DCM layer were below relationships obtained for the UML in summer, but coincided with those for winter phytoplankton (Churilova et al., 2017). Both values of $a_{ph}^*(\lambda)$ in the blue part of spectrum and R were significantly lower in the DCM than in the UML in summer. This likely results from a lower ratio of accessory pigments (mainly photoprotective) to chlorophyll *a* in phytoplankton responding to vertical gradients in environmental conditions, mainly light intensity (Churilova et al., 2017; Lutz, Sathyendranath, Head, & Li, 2003; MacIntyre, Kana, Anning, & Geider, 2002). The $A(\lambda)$ spectral coefficients of the absorption parameterization for the DCM layer coincided with those for winter phytoplankton across the spectrum, except in the 500–570 nm domain, where local peaks in absorption spectra were detected in the DCM layer. The coefficient and spectral shape of phytoplankton light

absorption changed systematically with depth (Figure 4). The spectral shapes in the DCM were characterized by local peaks at ~550 nm and a shoulder at ~490 nm, which became more pronounced with depth (Figure 4). The environmental conditions in the DCM layer are close to those in winter. The temperature in the BTC is similar to temperature in the UML in winter (Ivanov & Belokopytov, 2011). The phytoplankton in the DCM layer likely experience a supply of "new" nutrients, as it has been shown that the DCM is located just above the nitracline (Finenko et al., 2005) and a mechanism has been described that could provide DCM phytoplankton with upward fluxes of inorganic nitrogen and phosphorus (Krivenko & Parkhomenko, 2015). In our research the Flu and PAR profiles measured in June 1996 and in October 2005 as well as Flu profiles with assessment of $Z_{eu}$ in May 2016 (Figure 3) showed that the DCM was located near the depths with ~1% PAR. Taking into account that daily levels of PAR incident on the sea surface is ~56 E/m$^2$/d in May, ~58 E/m$^2$/d in June, ~51 E/m$^2$/d in August, ~35 E/m$^2$/d in September and ~32 E/m$^2$/d in October (Suslin, Korolev, Kucheryaviy, Churilova, & Krivenko, 2015), the irradiance at the DCM (at the DCM peak) will be ~0.56 E/m$^2$/d in May, ~0.58 E/m$^2$/d in June, ~0.51 E/m$^2$/d in August, ~0.35 E/m$^2$/d in September and ~0.32 E/m$^2$/d in October. Light intensity in the UML in winter, when the UML was comparable with $Z_{eu}$, was in a range 1.2–8.6 E/m$^2$/d and averaged 2.4 ± 0.8 E/m$^2$/d (Churilova et al., 2017). Consequently, phytoplankton in the DCM layer existed under lower light intensity than in winter. Because of an acclimation response to this low level of irradiance in the DCM layer, the C/Chl ratio (~4–28 mg/mg) was lower than that obtained for the winter phytoplankton (~25–40 mg/mg) (Churilova et al., 2017). As expected from the "package effect" (Morel & Bricaud, 1981) associated with increased intracellular pigment concentrations, values of $a_{ph}^*(\lambda)$ were lower than those obtained in winter the UML (Churilova et al., 2017). However, the expected decrease of $a_{ph}^*(\lambda)$ in the DCM layer compared to winter data was not observed (Figure 5), likely due to the high abundance of picocyanobacteria in the DCM. The picocyanobacteria contribution to total phytoplankton biomass was more than 10-fold higher in the DCM (Figure 7) than in the UML. In June 1996 and October 2005, the vertical gradient in the pico-fraction of the total phytoplankton biomass showed that picoplankton abundance increased and $B_{pico}$ reached in the DCM layer ~23 and ~41% on average in 1996 and 2005, correspondingly (Figure 7). Because increasing intracellular pigment concentration and decreasing cell size impact the "pigment package effect" in opposite ways (Morel & Bricaud, 1981), the $a_{ph}^*(678)$ values differed very little (~15%)
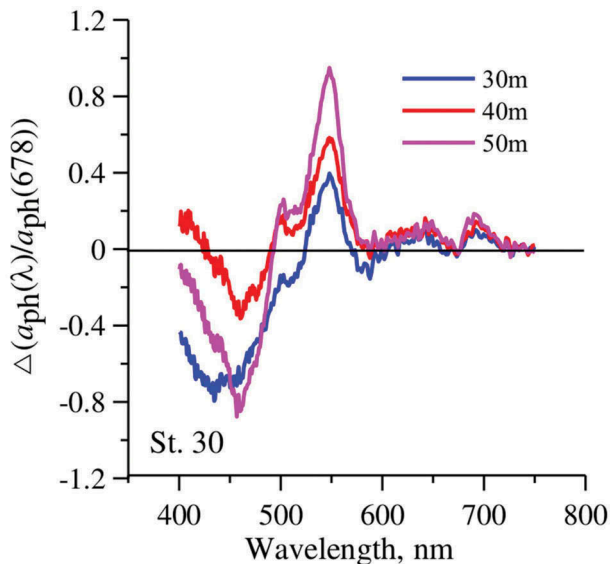
**Figure 9.** The difference ($\Delta(a_{ph}(\lambda)/a_{ph}(678))$) in spectral composition of absorption spectra ($a_{ph}(\lambda)$) between the sea surface and each of the depths 30 m, 40 m, and 50 m (st.30, October 2005). Each spectrum was first normalized to $a_{ph}(\lambda)$ at the red peak (678 nm).

from the values in the summer UML and also compared well with winter values (Churilova et al., 2017) (Figure 5).

Despite similarities in $a_{ph}^{*}(678)$ amplitude, there was a significant difference in the shape of absorption spectra between the DCM layer and the UML in both winter and summer (Figure 4). In the DCM layer, a shoulder at ~490 nm and a local maximum at ~550 nm are typical and likely indicative of absorption by phycourobilin (PUB) and phycoerythrobilin (PEB) (Six et al., 2007), which are pigment markers for the cyanobacteria *Synechoccocus* spp. (Moore, Georicke, & Chisholm, 1995; Palenik, 2001; Six et al., 2007). In our study cyanobacteria were detected within the water column from the surface to ~70 m, but their abundance was depth-dependent (Figure 7, 8). Observations from different years and from spring to autumn indicate that, during the seasonal stratification, the maximum of cyanobacteria abundance ($N_{pico}$) was in the lower part of the euphotic zone at a depth of 25–60 m. $N_{pico}$ at these depth reached ~$10^{10}$–$10^{11}$ cells/m$^3$ at particular stations. The increase in cyanobacteria abundance started underneath the layer of maximum temperature gradient and extended down almost to the depths where ~0.1% of sea-surface irradiance penetrated. Observed $N_{pico}$ variability in the surface layer and the features of its vertical distribution agreed with the results of previous investigations in the Black Sea (Rat'kova, 1989; Senichkina et al., 1991; Shalapyonok & Shalapyonok, 1997; Uysal, 2000). Comparison of phytoplankton data obtained in June 1996 and Autumn 2005 showed that in spite of the difference in the cyanobacteria abundance and total

phytoplankton biomass, the cyanobacteria vertical profiles had common features: the contribution of cyanobacteria in the total biomass increased below the TC, reaching a maximum near the bottom of euphotic zone at depths of 1–0.1% PAR (Figure 7). The vertical localization of the maximum in relative abundance of cyanobacteria ($B_{pico}$) is associated with light conditions near the bottom of the euphotic zone.

To quantitatively summarize depth-dependent change in $a_{ph}(\lambda)$, spectral shape difference spectra were computed for surface compared to each of the depths 30, 40, and 50 m (st30 in October 2005). To facilitate shape comparisons, each spectrum was first normalized at 678 nm (Figure 9). This approach emphasized the shoulder at ~490 nm and local maximum at ~550 nm that were more prevalent with increasing depth (Figure 9). An increased capacity of phytoplankton to absorb light in the spectrum region from ~480 to ~590 nm matches well with the blue-green light penetrating to the bottom of euphotic zone in the Black Sea (Vazyulya & Sheberstov, 2017). This light absorbing capacity markedly increased from 30 m (~1% PAR) to 50 m (~0.1% PAR). The high absorption capacity detected at blue-green wavelengths in the DCM emphasizes that the high abundance of PUB- and PEB-containing *Synechococcus* spp (Six et al., 2007) confers a light absorption advantage on DCM phytoplankton communities. These Black Sea results are consistent with previous suggestions that optical parameters are important niche dimensions for marine *Synechococcus* (Moore et al., 1995; Wood, Phinney, & Yentsch, 1998).

## Conclusions

Significant difference in phytoplankton light absorption properties ($a_{ph}^{*}(\lambda)$ magnitude and shape) between the UML and the DCM layer result from physiological acclimation on the cellular level and adaptive changes in species and size structure of phytoplankton communities. In the Black Sea, seasonal water stratification means the phytoplankton in the DCM layer experience specific environmental conditions compared to the UML: low temperature, high nutrient availability and blue-green irradiance with low intensity. These conditions lead to increased intracellular Chl-$a$ concentration and decreased accessory pigment (mainly photoprotective) concentrations as phytoplankton respond on a cellular level. Both low levels of irradiance, and its spectral quality (relatively enhanced in the range ~490–590 nm) near the bottom of $Z_{eu}$ are likely to be key factors associated with the increased prevalence of the picocyanobacteria *Synechococcus* spp in DCM phytoplankton communities near the bottom of $Z_{eu}$. In the DCM layer, low $a_{ph}^{*}(\lambda)$ values and the appearance of a shoulder

at ~490 nm and local maximum at ~550 nm are caused by changes in the pigment composition and concentrations in the cells, as well as by the abundance of cyanobacteria.

The parameterization of light absorption by phytoplankton in the DCM layer resulted from this study will make it possible to refine spectral models of downwelling radiance (Churilova et al., 2009) and primary production (Churilova & Suslin, 2010) in the Black Sea. This parameterization is a noteworthy improvement because it accounts for environment-specific acclimative and adaptive responses of phytoplankton communities, including changes in intracellular pigment concentrations, species composition, and size structure.

This study has revealed that particular phytoplankton light absorption properties ($a_{ph}^*(\lambda)$ magnitude and shape) are associated with dominance of the picocyanobacteria *Synechococcus* spp. Furthermore, shifts to *Synechococcus* dominance are associated with seasonal water stratification when the thermocline "locks" the phytoplankton near the bottom of the euphotic zone. These patterns in species/size structure of the phytoplankton community and its light absorption capacity in the deep euphotic layer (below the thermocline) were observed across an approximately 20-year period and in different Black Sea regions (including coastal waters) whenever stratification appeared within the euphotic layer (Berseneva & Churilova, 2001). Consequently, these patterns of change in the structural and functional characteristics of the deep phytoplankton community are general features for the Black Sea, at least when conditions of seasonal stratification of waters within the euphotic zone are observed. Coastal waters, with their relatively high temporal variability in mixing and associated loss of stratification, require additional consideration; which would be a subject of future investigations.

## Acknowledgments

## Disclosure statement

No potential conflict of interest was reported by the authors.

## ORCID

T. Churilova 🔄 http://orcid.org/0000-0002-0045-7284
V. Suslin 🔄 http://orcid.org/0000-0002-8627-7603
H.M. Sosik 🔄 http://orcid.org/0000-0002-4591-2842
S. Moncheva 🔄 http://orcid.org/0000-0002-4213-2111

## References

Babin, M., Stramski, D., Ferrari, G.M., Claustre, H., Bricaud, A., Obolensky, G., & Hoepffner, N. (2003). Variations in the light absorption coefficients of phytoplankton, nonalgal particles, and dissolved organic matter in coastal waters around Europe. *Journal of Geophysical Research*, 108(C7), 3211. doi:10.1029/2001JC000882

Behrenfeld, M.J., Boss, E., Siegel, D.A., & Shea, D.M. (2005). Carbon-based ocean productivity and phytoplankton physiology from space. *Global Biogeochemical Cycles*, 19, GB1006. doi:10.1029/2004GB002299

Behrenfeld, M.J., O'Malley, R.T., Siegel, D.A., McClain, C. R., Sarmiento, J.L., Feldman, G.C., ... Boss, E.S. (2006). Climate-driven trends in contemporary ocean productivity. *Nature*, 444(7120), 752–755. doi:10.1038/nature05317

Berseneva, G., & Churilova, T. (2001). Chlorophyll concentration and phytoplankton optical characteristics in shelf waters of the Black Sea near the Crimea. *Marine Hydrophysical Journal*, 2, 44–57 (in Russian).

Berthon, J.-F., Mélin, F., & Zibordi, G. (2008). Ocean Colour Remote Sensing of the Optically Complex European Seas. In V. Barale & M. Gade (Eds.), *Remote Sensing of the European Seas* (pp. 35–52). Berlin/Heidelberg, Germany: Springer Science-Business Media B.V.

Bricaud, A., Babin, M., Morel, A., & Claustre, H. (1995). Variability in the chlorophyll-specific absorption coefficients of natural phytoplankton: Analysis and parameterization. *Journal of Geophysical Research*, 100(C7), 13321–13332. doi:10.1029/95JC00463

Bricaud, A., Morel, A., Babin, M., Allali, K., & Claustre, H. (1998). Variations of light absorption by suspended particles with chlorophyll a concentration in oceanic (case 1) waters: Analysis and implications for bio-optical models. *Journal of Geophysical Research*, 103(C13), 31033–31044. doi:10.1029/98JC02712

Chami, M., Shybanov, E., Churilova, T., Khomenko, G., Lee, M., Martynov, O., ... Korotaev, G. (2005). Optical properties of the particles in the Crimea coastal waters (Black Sea). *Journal of Geophysical Research*, 110 (C11020), 1–17. doi:10.1029/2005JC003008

Churilova, T. (2001). Light absorption by phytoplankton and detritus in the Black Sea in spring. *Oceanolog*, 41(5), 687–695.

Churilova, T., & Berseneva, G. (2004). Absorption of light by phytoplankton, detritus, and dissolved organic substances in the coastal region of the Black Sea (July–

August 2002). *Physical Oceanography*, 14, 221–233. doi:10.1007/s11110-005-0016-3

Churilova, T., Berseneva, G., & Georgieva, L. (2004). Variability in bio-optical characteristics of phytoplankton in the Black Sea. *Oceanology*, 44(2), 192–204.

Churilova, T., & Suslin, V. (2010) Parameterization of light absorption by all in-water optically active components in the Black Sea: Impact for underwater irradiance and primary production modelling. In *Coastal to Global Operational Oceanography: Achievements and Challenges: Proceedings of the fifth international conference on EuroGOOS, 28* (pp. 199–205). Exeter, UK: EuroGOOS Publication.

Churilova, T., Suslin, V., Krivenko, O., Efimova, T., Moiseeva, N., Mukhanov, V., & Smirnova, L. (2017). Light Absorption by Phytoplankton in the Upper Mixed Layer of the Black Sea: Seasonality and Parametrization. *Frontiers in Marine Science*, 4(90). doi:10.3389/fmars.2017.00090

Churilova, T., Suslin, V., & Sosik, H.M. (2009). A spectral model of underwater irradiance in the Black Sea. *Physical Oceanography*, 19(6), 366–378. doi:10.1007/s11110-010-9060-8

Cleveland, J.S. (1995). Regional models for phytoplankton absorption as a function of chlorophyll a concentration. *Journal of Geophysical Research*, 100(C7), 13333–13344. doi:10.1029/95JC00532

Dmitriev, E., Khomenko, G., Chami, M., Sokolov, A., Churilova, T., & Korotaev, G. (2009). Parameterization of light absorption by components of seawater in optically complex coastal waters of the Crimea Peninsula (Black Sea). *Applied Optics*, 48(7), 1249–1261. doi:10.1364/AO.48.001249

Finenko, Z., Churilova, T., & Lee, R. (2005). Dynamics of the vertical distributions of chlorophyll and phytoplankton biomass in the Black Sea. *Oceanology*, 4(1), 112–126.

Fujiki, T., & Taguchi, S. (2002). Variability in chlorophyll a specific absorption coefficient in marine phytoplankton as a function of cell size and irradiance. *Journal of Plankton Research*, 24(9), 859–874. doi:10.1093/plankt/24.9.859

Georgieva, L.V. (1993). Species composition of phytoplankton communities. In A.V. Kovalev & Z.Z. Finenko (Eds.), *Plankton of the Black Sea* (pp. 33–55). Kiev: Naukova Dumka. (in Russian).

Hoepffner, N., & Sathyendranath, S. (1992). Bio-optical characteristics of coastal waters: Absorption spectra of phytoplankton and pigment distribution in the western North Atlantic. *Limnology and Oceanography*, 37, 1660–1679. doi:10.4319/lo.1992.37.8.1660

Holm-Hansen, O., Lorenzen, C.J., Holmes, R.W., & Strickland, J.D.H. (1965). Fluorometric determination of chlorophyll. *Journal Cons Institute Explor Mer*, 30, 3–15. doi:10.1093/icesjms/30.1.3

Ivanov, V.A., & Belokopytov, V.N. (2011). *Oceanography of the Black Sea*. Sevastopol: National Academy of Science of Ukraine, Marine Hydrophysical Institute.

Jeffrey, S.W., & Humphrey, G.F. (1975). New spectrophotometric equations for determining chiorophylls a, b, c1 and c2 in higher plants, algae and phytoplankton. *Biochemical Physiological Pflanzen (BPP)*, 167, 191–197. doi:10.1016/S0015-3796(17)30778-3

Kirk, J.T.O. (2011). *Light and photosynthesis in aquatic ecosystems* (3rd ed.). Cambridge, UK: Cambridge University Press.

Kishino, M., Takahashi, N., Okami, N., & Ichimura, S. (1985). Estimation of the spectral absorption coefficients of phytoplankton in the sea. *Bulletin of Marine Science*, 37, 634–642.

Kopelevich, O.V., Burenkov, V.I., Ershova, S.V., Sheberstov, S.V., & Evdoshenko, M.A. (2004). Application of SeaWiFS data for studing variability of bio-optical characteristics in the Barents, Black and Caspian Seas. *Deep-Sea Research. Part II: Tropical Studies in Oceanography*, 51(10–11), 1063–1091. doi:10.1016/S0967-0645(04)00101-8

Kopelevich, O.V., Sheberstov, S.V., Burenkov, V.I., Vazyulya, S.V., & Likhacheva, M.V. (2007). Assessment of underwater irradiance and absorption of solar radiation at water column from satellite data. In *Proceedings of SPIE - The International Society for Optical Engineering Current Research on Remote Sensing, Laser Probing, and Imagery in Natural Waters. Iss. "Current Research on Remote Sensing, Laser Probing, and Imagery in Natural Waters" sponsors:* SPIE Russia Chapter. C. 661507. St. Petersburg, RF: Nauka

Krivenko, O.B., & Parkhomenko, A.B. (2015). Upward and regeneration fluxes of inorganic nitrogen and phosphorus of the deep-water areas of the Black Sea. *Biology Bulletin Reviews*, 5(3), 268–281. doi:10.1134/S2079086415030044

Lorenzen, C.J. (1967). Determination of chlorophyll and pheopigments: Spectrophotometric equations. *Limnology and Oceanography*, 12, 343–346. doi:10.4319/lo.1967.12.2.0343

Lutz, V.A., Sathyendranath, S., & Head, E.J.H. (1996). Absorption coefficient of phytoplankton: Regional variations in the North Atlantic. *Marine Ecology Progress Series*, 135, 197–213. doi:10.3354/meps135197

Lutz, V.A., Sathyendranath, S., Head, E.J.H., & Li, W.K.W. (2003). Variability in pigment composition and optical characteristics of phytoplankton in the Labrador Sea and the Central North Atlantic. *Marine Ecology Progress Series*, 260, 1–18. doi:10.3354/meps260001

MacIntyre, H.L., Kana, T.M., Anning, J., & Geider, R. (2002). Photoacclimation of photosynthesis irradiance response curves and photosynthetic pigments in microalgae and cyanobacteria. *Journal of Phycology*, 38, 17–38. doi:10.1046/j.1529-8817.2002.00094.x

MacIsaac, E.A., & Stockner, J.G. (1993). Enumeration of phototrophic picoplankton by autofluorescence microscopy. In P.F. Kemp, B.F. Sherr, E.B. Sherr, & J.J. Cole (Eds.), *Handbook of methods in aquatic microbial ecology* (pp. 187–197). Boca Raton, Fla: Lewis Publishers.

Marie, D., Partensky, F., Vaulot, D., & Brussaard, C.P.D. (1999). Enumeration of phytoplankton, bacteria and viruses in marine samples. In J.P. Robingson, Z. Darzynkiewicz, P.N. Dean, A. Orfao, P. Rabinovitch, C. C. Stewart, & L.L. Wheless (Eds.), *Current protocols in cytometry: Supplement 10, Unit 11.11*. New York: John Wiley and Sons Inc.

Mitchell, B.G. (1990, September). Algorithms for determining the absorption coefficient of aquatic particulates using the quantitative filter technique (QFT). In R. Spinrad (Eds.), *Ocean Optics X* (pp. 137–148). Bellingham, Washington: SPIE.

Mitchell, B.G., Kahru, M., Wieland, J., & Stramska, M. (2003). Determination of spectral absorption coefficients of particles, dissolved material and phytoplankton for discrete water samples. In J.L. Mueller, G.S. Fargion, & C.R. McClain (Eds.), *Ocean Optics Protocols for Satellite Ocean Color Sensor Validation: Revision 4, Vol. IV. Inherent Optical Properties: Instruments, Characterizations, Field Measurements and Data Analysis Protocols* (pp. 39–64). Greenbelt, Maryland: NASA Goddard Space Flight Center.

Mitchell, B.G., & Kiefer, D.A. (1988). Chlorophyll a specific absorption and fluorescence excitation spectra for light limited phytoplankton. *Deep-Sea Research*, 35(5), 639–663. doi:10.1016/0198-0149(88)90024-6

Moore, L.R., Georicke, R., & Chisholm, S.W. (1995). Comparative physiology of Synechococcus and Prochlorococcus: Influence of light and temperature on growth, pigments, fluorescence and absorptive properties. *Marine Ecology Progress Series*, 116, 259–275. doi:10.3354/meps116259

Morel, A. (1991). Light and marine photosynthesis: A spectral model with geochemical and climatological implications. *Progress in Oceanography*, 26, 263–306. doi:10.1016/0079-6611(91)90004-6

Morel, A., & Bricaud, A. (1981). Theoretical results concerning light absorption in a discrete medium, and application to specific absorption of phytoplankton. *Deep-Sea Research*, 28, 1375–1393. doi:10.1016/0198-0149(81)90039-X

O'Reilly, J.E., Maritorena, S., O'Brien, M.C., Siegel, D.A., Toole, D., Menzies, D., … Culver, M. (2000). NASA Techical Memorandum.Vol.11, SeaWiFS Postlaunch Calibration and Validation Analyses, Part 3. 49 pp. In S.B. Hooker & E.R. Firestone (Eds.), *SeaWiFS Postlaunch Technical Report Series*. Greenbelt, Maryland: NASA Goddard Space Flight Center.

Palenik, B. (2001). Chromatic Adaptation in Marine Synechococcus Strains. *Applaied and Environmental Microbiology*, 67(2), 991–994.

Rat'kova, T.N. (1989). The phytoplankton of the open areas of the Black Sea. In M.E. Vinogradov & M.V. Flint (Eds.), *Structure and productive characters of planktonic communities of the Black Sea* (pp. 38–53). Moscow: Nauka. (in Russian).

Saba, V.S., Friedrichs, M.A.M., Antoine, D., Armstrong, R. A., Asanuma, I., Behrenfeld, M.J., … Westberry, T.K. (2011). An evaluation of ocean color model estimates of marine primary productivity in coastal and pelagic regions across the globe. *Biogeosciences*, 8, 489–503. doi:10.5194/bg-8-489-2011

Schapira, M., Buscot, M.-J., Pollet, T., Leterme, S.C., & Seuront, L. (2010). Distribution of picophytoplankton communities from brackish to hypersaline waters in a South Australian coastal lagoon. *Saline Systems*, 6, 2–16. doi:10.1186/1746-1448-6-2

Senichkina, L.G., Georgieva, L.V., Nesterova, D.A., Fashchuk, D.Y., & Lifshiz, A.V. (1991). Phytoplankton of the Black Sea in summer period, 1989: biomass and connection with hydrological conditions. In M.E. Vinogradov (Ed.), *Variability of the Black Sea ecosystem: Natural and anthropogenic factors* (pp. 104–116). Moscow: Nauka. (in Russian).

Shalapenok, L.S., & Shalapenok, A. (1997). Heterogeneous pigment composition of phycoerytrin-conyaining picocyanobacteria Synechococcus spp. in the Black Sea. *Mikrobiologiya*, 66, 80–84.

Six, C., Thomas, J.-C., Garczarek, L., Ostrowski, M., Dufresne, A., Blot, N., … Partensky, F. (2007). Diversity and evolution of phycobilisomes in marine Synechococcus spp.: A comparative genomics study. *Genome Biology*, 8, R259. doi:10.1186/gb-2007-8-12-r259

Sosik, H.M., & Mitchell, B.G. (1991). Absorption, fluorescence and quantum yield for growth in nitrogen-limited *Dunaliella tertiolecta. Limnology and oceanography*, 36, 910–921.

Sosik, H.M., & Mitchell, B.G. (1994). Effects of temperature on growth and light absorption in *Dunaliella tertiolecta. Journal of phycology*, 30, 833–840. doi:10.1111/j.0022-3646.1994.00833.x

Sosik, H.M., & Mitchell, B.G. (1995). Light absorption by phytoplankton, photosynthetic pigments and detritus in the California Current System. *Deep Sea-Research*, 42, 1717–1748. doi:10.1016/0967-0637(95)00081-G

Suslin, V., & Churilova, T. (2016). The Black Sea regional algorithm of separation of light absorption by phytoplankton and colored detrital matter using ocean color scanner's bands from 480-560 nm. *International Journal of Remote Sensing*, 37(18), 4380–4400. doi:10.1080/01431161.2016.1211350

Suslin, V.V., Churilova, T.Y.A., Lee, M., Moncheva, S., & Finenko, Z.Z. (2018). *Comparison of the Black Sea chlorophyll-a algorithms for SeaWiFS and MODIS instruments. Fundamentalnaya i Prikladnaya Gidrofizika*, 11(3), 64—72. doi: 10.7868/S2073667318030085. (In Russian).

Suslin, V.V., Korolev, S.N., Kucheryaviy, A.A., Churilova, T.Y. A., & Krivenko, O.V. (2015, November). Photosynthetically available radiation on surface of the Black Sea based on ocean color data. In *Proceedings of SPIE 9680 21st International Symposium Atmospheric and Ocean Optics: Atmospheric Physics*. Tomsk, RF. doi: 10.1117/12.2203660.

Suzuki, K., Kishino, M., Sasaoka, K., Saitoh, S.I., & Saino, T. (1998). Chlorophyll-Specific Absorption Coefficients and Pigments of Phytoplankton off Sanriku, Northwestern North Pacific. *Journal of Oceanography*, 54, 517–526. doi:10.1007/BF02742453

Tassan, S., & Ferrari, G. (1995). An alternative approach to absorption measurements of aquatic particles retained on filters. *Limnology and Oceanography*, 40(8), 1358–1368. doi:10.4319/lo.1995.40.8.1358

Uysal, Z. (2000). Pigments, size and distribution of Synechococcus spp. In the Black Sea. *Journal of Marine Systems*, 24, 313–326. doi:10.1016/S0924-7963(99)00092-5

Vazyulya, S.V., & Sheberstov, S.V. (2017). Secondary processing of field measurements data of spectral underwater irradiance in the visible range. In *Proceeding of IX International conference "Current Problems in Optics of Natural Waters"* (pp. 229–234). St. Petersburg. (in Russian).

Vedernikov, V.I. (1989). Primary production and chlorophyll in the Black Sea in summer and fall. In M.E. Vonogradov & M.V. Flint (Eds.), *Struktura i produktsionnye kharakteristiki planktonnykh soobshchestv: Sbornikh nauchnykh rabot* (pp. 65–83). Moscow: Nauka. (in Russian).

Wood, M., Phinney, D.A., & Yentsch, C.S. (1998). Water column transparency and the distribution of spectrally distinct forms of phycoerythrincontaining organisms. *MEPS*, 162, 25–31. doi:10.3354/meps162025

Yentsch, C.S. (1962). Measurement of visible light absorption by particulate matter in the ocean. *Limnology and Oceanography*, 7, 207–217. doi:10.4319/lo.1962.7.2.0207

Yunev, O.A., Moncheva, S., & Carstensen, J. (2005). Longterm variability of vertical chlorophyll a and nitrate profiles in the open Black Sea: Eutrophication and climate change. *MEPS*, 294, 95–107. doi:10.3354/meps294095